

REPORT DOCUMENTATION PAGE

*Form Approved
OMB No. 0704-0188*

Public reporting burden for this collection of information is estimated to average 1 hour per response, including the time for reviewing instructions, searching existing data sources, gathering and maintaining the data needed, and completing and reviewing this collection of information. Send comments regarding this burden estimate or any other aspect of this collection of information, including suggestions for reducing this burden to Department of Defense, Washington Headquarters Services, Directorate for Information Operations and Reports (0704-0188), 1215 Jefferson Davis Highway, Suite 1204, Arlington, VA 22202-4302. Respondents should be aware that notwithstanding any other provision of law, no person shall be subject to any penalty for failing to comply with a collection of information if it does not display a currently valid OMB control number. PLEASE DO NOT RETURN YOUR FORM TO THE ABOVE ADDRESS.

1. REPORT DATE (DD-MM-YYYY)		2. REPORT TYPE Technical Papers		3. DATES COVERED (From - To)	
4. TITLE AND SUBTITLE				5a. CONTRACT NUMBER	
				5b. GRANT NUMBER	
				5c. PROGRAM ELEMENT NUMBER	
6. AUTHOR(S)				5d. PROJECT NUMBER <i>2308</i>	
				5e. TASK NUMBER <i>M19B</i>	
				5f. WORK UNIT NUMBER <i>346 058</i>	
7. PERFORMING ORGANIZATION NAME(S) AND ADDRESS(ES)				8. PERFORMING ORGANIZATION REPORT	
Air Force Research Laboratory (AFMC) AFRL/PRS 5 Pollux Drive Edwards AFB CA 93524-7048					
9. SPONSORING / MONITORING AGENCY NAME(S) AND ADDRESS(ES)				10. SPONSOR/MONITOR'S ACRONYM(S)	
Air Force Research Laboratory (AFMC) AFRL/PRS 5 Pollux Drive Edwards AFB CA 93524-7048				11. SPONSOR/MONITOR'S NUMBER(S) <i>Please see attached</i>	
12. DISTRIBUTION / AVAILABILITY STATEMENT					
Approved for public release; distribution unlimited.					
13. SUPPLEMENTARY NOTES					
14. ABSTRACT					
<i>20030205 289</i>					
15. SUBJECT TERMS					
16. SECURITY CLASSIFICATION OF:			17. LIMITATION OF ABSTRACT <i>A</i>	18. NUMBER OF PAGES	19a. NAME OF RESPONSIBLE PERSON Leilani Richardson
a. REPORT Unclassified	b. ABSTRACT Unclassified	c. THIS PAGE Unclassified			19b. TELEPHONE NUMBER (include area code) (661) 275-5015

MEMORANDUM FOR PRS (In-House Publication)

FROM: PROI (STINFO)

15 August 2001

SUBJECT: Authorization for Release of Technical Information, Control Number: AFRL-PR-ED-TP-2001-171

Andrew D. Ketsdever, Brian M. Eccles (USC), "Fiber Optic Sensors for the Study of S/C-Thruster
Interactions: Ion Sputtering"

Journal of Spacecraft & Rockets
(Deadline: N/A)

(Statement A)

1. This request has been reviewed by the Foreign Disclosure Office for: a.) appropriateness of distribution statement, b.) military/national critical technology, c.) export controls or distribution restrictions, d.) appropriateness for release to a foreign nation, and e.) technical sensitivity and/or economic sensitivity.

Comments: _____

Signature _____ Date _____

2. This request has been reviewed by the Public Affairs Office for: a.) appropriateness for public release and/or b) possible higher headquarters review.

Comments: _____

Signature _____ Date _____

3. This request has been reviewed by the STINFO for: a.) changes if approved as amended, b) appropriateness of references, if applicable; and c.) format and completion of meeting clearance form if required

Comments: _____

Signature _____ Date _____

4. This request has been reviewed by PR for: a.) technical accuracy, b.) appropriateness for audience, c.) appropriateness of distribution statement, d.) technical sensitivity and economic sensitivity, e.) military/national critical technology, and f.) data rights and patentability

Comments: _____

APPROVED/APPROVED AS AMENDED/DISAPPROVED

PHILIP A. KESSEL
Technical Advisor
Space and Missile Propulsion Division

Date

Fiber Optic Sensors for the Study of Spacecraft-Thruster Interactions: Ion Sputtering

Andrew D. Ketsdever[†]
Air Force Research Laboratory

Brian M. Eccles^{*}
University of Southern California

INTRODUCTION

The interaction between thruster effluents and spacecraft surfaces has received considerable attention recently. Historically, thruster interaction concerns have focused on self-contamination from non-direct and high angle (measured from the thruster centerline) plume impingement. The growing popularity of distributed networks of cooperative, co-orbiting satellite clusters has brought about an additional need to address direct plume impingement or cross-contamination. Typically, quartz crystal microbalances (QCMs) are used to investigate spacecraft-thruster interactions where the major contamination mechanism is the adsorption of molecular species on critical surfaces.¹ New methods are required to investigate the complex nature of plume impingement from advanced ion electric thrusters where the major interaction is the sputtering of critical surfaces. Additionally, QCMs are limited in that they only provide interaction data at a single point; however, the plume characteristics of a typical ion thruster can vary several orders of magnitude over short distances. This study focuses

when was
is paper
approved?
INFO has
approval
and, is it
der or
different title
author?

* Presented as paper 2001-2958 at the AIAA 35th Thermophysics Conference, Anaheim, CA, 11-14 June 2001.

[†] Senior Research Engineer, Propulsion Directorate, Aerophysics Branch, Edwards AFB, CA 93524, AIAA Senior Member.

* Undergraduate Student, Department of Aerospace and Mechanical Engineering, Los Angeles, CA 90089-1191, AIAA Student Member

Distribution Statement A: Approved for Public Release; Distribution Unlimited.

on the proof-of-principle demonstration of a fiber optic contamination sensor (FOCS), which can provide a complete interaction map for ion thrusters as an alternative to QCMs. The FOCS measures the depletion of light transmitted through the fiber as the cladding material is removed (sputtered) by energetic plume ions. Although this work is primarily concerned with assessing the FOCS for highly energetic ion interactions that induce material sputtering, the sensor may also be appropriate as an adsorption monitor for molecular contaminants.²

THRUSTER
NOT
THRU

FOCS Principle of Operation

The difference in the index of refraction between the core and cladding is responsible for propagating the light signal through the optical fiber. Although the light traveling in the fiber can be thought of as undergoing total internal reflection at the core-cladding boundary, a fraction of the light, referred to as the evanescent wave, actually penetrates into the cladding before being reflected back into the core.³ The characteristic penetration length of the evanescent wave is defined as the distance at which the intensity drops to e^{-1} of its initial intensity (at the core-cladding boundary), and is given by

$$\beta^{-1} = \frac{\lambda}{2n_{\text{clad}}} (n_{\text{core}}^2 - n_{\text{clad}}^2)^{-\frac{1}{2}}, \quad (1)$$

where λ is the transmitted wavelength, and n_{core} and n_{clad} are the indices of refraction for the core and cladding material, respectively. The intensity of the evanescent wave decreases exponentially with increased distance from the core-cladding interface. If the core is sufficiently eccentric, the tail of the evanescent wave extends beyond the cladding into the surrounding environment. This condition is representative of light propagation through the sputtered (or etched) cladding of an optical fiber where the thickness on one side of the core has been significantly reduced. As the sputtering process continues, more of the evanescent tail would be exposed to the sensor environment, causing a decrease in the transmitted signal strength. The rate of decrease would be proportional to the sputter rate and could conceivably be calibrated to allow for the estimation of energetic ion flux at the sensor location.

EXPERIMENTAL SET UP: SIMULATED ION SPUTTERING

"Setup" is one word, not two

Is kept
using
corresponding
paragraph

In order to simulate the effects of xenon ion sputtering on optical fiber, the fiber was etched in an acid solution. Hydrofluoric acid (HF) was used, due to its strong reaction with silicon dioxide. The primary goal of this experiment was to observe the decrease in transmitted light level as a function of the optical fiber cladding thickness during the etching. Corning® SMF-28™ single-mode fiber was used, which consisted of a $8.2 \mu\text{m}$ diameter doped SiO_2 core, a $125 \mu\text{m}$ diameter pure SiO_2 cladding, and a $245 \mu\text{m}$ diameter acrylate protective coating. For light with a wavelength of 1550 nm , n_{core} and n_{clad} are 1.4505 and 1.4447, respectively.⁴ The $245 \mu\text{m}$ acrylate coating was removed from a 5 cm segment of the fiber using an acetone bath, exposing the cladding for HF_{aq} etching. The light signal was provided by a 1.6 mW, fiber coupled diode laser, which was determined to have an operating wavelength of 1304 nm . A Gallium-Arsenide (GaAs) infrared detector was coupled at the other end of the fiber to monitor the output signal. The exposed section of the fiber cladding was immersed in the HF_{aq} while the transmitted intensity was monitored as a function of time. The acid etched the circumference of the fiber evenly from all directions, which is physically different from energetic ion sputtering on only the surface facing the incident thruster plume. However, the results yielded proof-of-principle demonstration for the FOCS operation.

RESULTS

Figure 1 shows the laser light intensity as a function of time (i.e., cladding thickness) for optical fibers in 49% and 20% HF_{aq} solutions (by weight). The etch rate for the 49% HF_{aq} was estimated to be $1.6 \mu\text{m}/\text{min}$, which is similar to published results for silica.⁵ The etch rate for the 20% HF_{aq} was estimated to be $0.16 \mu\text{m}/\text{min}$. In Fig. 1, the intensity remains relatively constant until the fibers are etched to a diameter of approximately $21.3 \mu\text{m}$. This corresponds to a remaining cladding thickness of $6.55 \mu\text{m}$ or 5λ . From Eq. (2), the characteristic length of penetration, β^{-1} , of the laser light into the cladding material is approximately $3.5 \mu\text{m}$ or 2.7λ . As expected, the transmitted signal does not degrade until the cladding thickness approaches β^{-1} . The noise seen in the traces is most likely due to the fast etch

- Pls add
comma
where
indicated

rate, which is known to leave a rough surface.⁵ The repeatability of the data in Fig. 2 suggests that a fiber sensor used to investigate sputter removal of cladding material can be adequately calibrated. In order to make the experimental results meaningful for spacecraft contamination studies, it is necessary to correlate the measured HF_{aq} etch rate to an estimated ion sputter rate for some thruster.

ESTIMATED SPUTTERING RATES FOR HALL THRUSTERS

The SPT-100 Hall thruster is used in this study as a benchmark thruster since adequate experimental results for the thruster plume are reported in the literature. The sputter rate for SiO₂ impacted by the energetic plume of an SPT-100 has been obtained from two sources. First, Randolph⁶ et al. experimentally measured the sputter rate for a quartz engineering surface one meter downstream of the SPT-100 at various angles relative to the thruster centerline. Second, theoretical results for the sputter yield were obtained by the Transport of Ions in Matter (TRIM) computational model, which utilizes a Monte Carlo numerical approach with a fully quantum mechanical treatment of ion-atom collisions.⁷ The TRIM-derived sputter yields were then combined with SPT-100 plume characteristics experimentally obtained by King and Gallimore⁸ in order to estimate an ion sputter rate. The sputter rate at a given point in the plume for a material impacted by an energetic ion beam is given by

If possible, pls add →
the subscripted
"i" to the equation

$$\frac{dx}{dt} = \frac{\Phi(x, \phi) \bar{\gamma}(E_i, \theta)}{\rho}, \quad \bar{\gamma}(E) = \frac{\int_0^{\infty} f(E) \gamma(E) dE}{\int_0^{\infty} f(E) dE}, \quad (2)$$

where $\Phi(x, \phi)$ is the ion flux from the thruster at some axial (x) and radial (ϕ) location downstream of the exit plane [ions/cm² sec], $\bar{\gamma}(E_i, \theta)$ is the average sputter yield as a function of ion impact energy (E) and incident angle (θ), ρ is the number density of the sputtered material [atoms/cm³] and $f(E)$ is the ion energy distribution function at a given axial and radial position in the plume.

DISCUSSION: SENSOR UTILITY

pls keep
heading w/
corresponding
paragraph (next page)

Table 1 gives the sputter rates for a SiO_2 material surface impacted one meter downstream of an SPT-100, as determined both experimentally and numerically. The effect time is defined as the time required to remove the final 5λ of cladding thickness, as shown in Fig. 2 (i.e., the time needed to go from maximum to zero signal transmission through the optical fiber). The experimental results were obtained for a quartz surface oriented such that the ions were normally incident, or $\theta = 90^\circ$. The numerical results were calculated assuming that the incidence angle of the ions impacting the SiO_2 surface was the equal to the divergence angle from the thruster centerline, or $\theta = \phi$. For normally incident ions, the sputter rate is driven by the decrease in ion flux as the plume angle increases, since the sputter yield can be considered constant for a given energy. However, the numerical results show that when the sputtered surface is held perpendicular to the thruster centerline, such that $\theta = \phi$ the sputter rate does not drop off as quickly for higher divergence angles. This is due to the increased sputter yield at the corresponding higher incident angles counteracting the decrease in energetic ion flux. As shown in Table 1, the predicted effect time can vary greatly depending on the incident angle of the ions on the SiO_2 surface.

pls make
sure the per-
centage
shows up
after the
symbol

A potential configuration for FOCS monitoring of on-orbit spacecraft interactions can be envisioned as a two-dimensional grid of optical fibers installed on a critical surface such as a solar array panel. As a sensor system, multiple fibers can be connected to a single diode laser source and detector with coupling to allow independent measurement of a given fiber. At various locations of interest on the FOCS grid, the fiber cladding would be exposed to the spacecraft environment. Also, the amount of cladding removed prior to installation could be varied at different locations, which would allow contamination measurement in different phases of the spacecraft lifetime. This arrangement of sensors would allow the gathering of contamination data from the FOCS locations on the grid, thereby providing a more complete understanding of the spatial and temporal thruster interaction.

Again, pls → CONCLUSIONS
put heading
w/ corresponding
paragraph

The FOCS principle of operation has been verified in a proof-of-principle demonstration. A decrease in transmitted signal strength was observed as the optical fiber cladding thickness decreased during the HF_{aq} solution etch. The experimental results obtained in this study simulated the sputtering of optical fiber cladding material by energetic ions in the plume of ion electric thrusters. The repeatability of the HF_{aq} etch results indicate that the sensor can be calibrated for transmitted light intensity as a function of cladding thickness. Measured and calculated sputter rates for a SPT-100 plume impacting a SiO₂ surface were used to calculate values for the FOCS effect time based on correlations with the measured HF_{aq} etch characteristics. Results indicate that the transmitted light intensity will go from maximum to zero signal in approximately 6.5 hours if the sensor is placed one meter downstream of an SPT-100 on the thruster centerline. This effect time is shown to increase as the divergence angle from the thruster centerline increases. Placing the optical fiber perpendicular to the thruster centerline can reduce the predicted effect time at high plume angles. In the perpendicular configuration, effect times less than one-tenth of the design lifetime of a typical Hall thruster (~ 2000 hours) can be achieved for almost any plume angle.

← pls remove the "e"

REFERENCES

1. Spanjers, G., Schilling, J., Engelman, S., Bromaghim, D., Johnson, L., "Preliminary analysis of contamination measurements from the ESEX 26 kW ammonia arcjet flight experiment," AIAA paper 1999-2709, June 1999.
*s see
te on
ham of
ge 1*
2. Ketsdever, A., Eccles, B., Abid, M., Netherwood, G., Fitzpatrick, C., "Fiber Optic Sensors for the Study of Spacecraft-Thruster Interactions: Ion Sputtering," AIAA paper 2001-2958, June 2001.
3. Hecht, J., Understanding fiber optics, Third Edition, Prentice Hall, Upper Saddle River, NJ, pp. 64, 1999.
4. Corning, Inc. "Corning SMF-28 optical fiber: product information," P1036, April 2001.
5. Williams, K., Muller, R., "Etch rates for micromachining processing," *Journal of Microelectromechanical Systems*, Vol. 5, No. 4, pp. 256-269, December 1996.
6. Randolph, T., Pencil, E., Manzella, D., "Far-field plume contamination and sputtering of the stationary plasma thruster," AIAA paper 94-2855, June 1994.
7. Ziegler, J., Biersack, J., Littmark, U., The stopping and range of ions in solids, Pergamon Press, New York, NY, 1985.

← pls add the R where indicated
"PIR 1036"

8. King, L., Gallimore, A., "Ion energy diagnostics in the plume of an SPT-100 from thrust axis to backflow region," AIAA paper 98-3641, July 1998.

FIGURE CAPTIONS

Figure 1: Transmitted laser intensity as a function of time during 49% (Left side) and 20% (Right side) HF_{aq} etch of SiO_2 optical fiber cladding.

Figure 2: Transmitted laser intensity as a function of time during 20% HF_{aq} etch of SiO_2 optical fiber cladding. Repeatability of etch results shown for four separate optical fibers.

TABLE CAPTIONS

Table 1: Estimated sputter rates and corresponding effect times for FOCS one meter downstream of an SPT-100 Hall thruster.

ϕ (deg.)	$\theta = 90^\circ$		$\theta = \phi$	
	dx/dt^6 ($\mu\text{m}/\text{min}$)	Effect Time (hrs)	dx/dt ($\mu\text{m}/\text{min}$)	Effect Time (hrs)
0			1.68E-02	6.5
15	1.03E-02	10.6	-	-
30	2.00E-03	54.3	8.55E-04	127.1
45	6.18E-04	175.8	-	-
60	6.06E-05	1793.2	8.28E-04	131.2
80	6.90E-06	15749	5.52E-04	196.9

Table 1

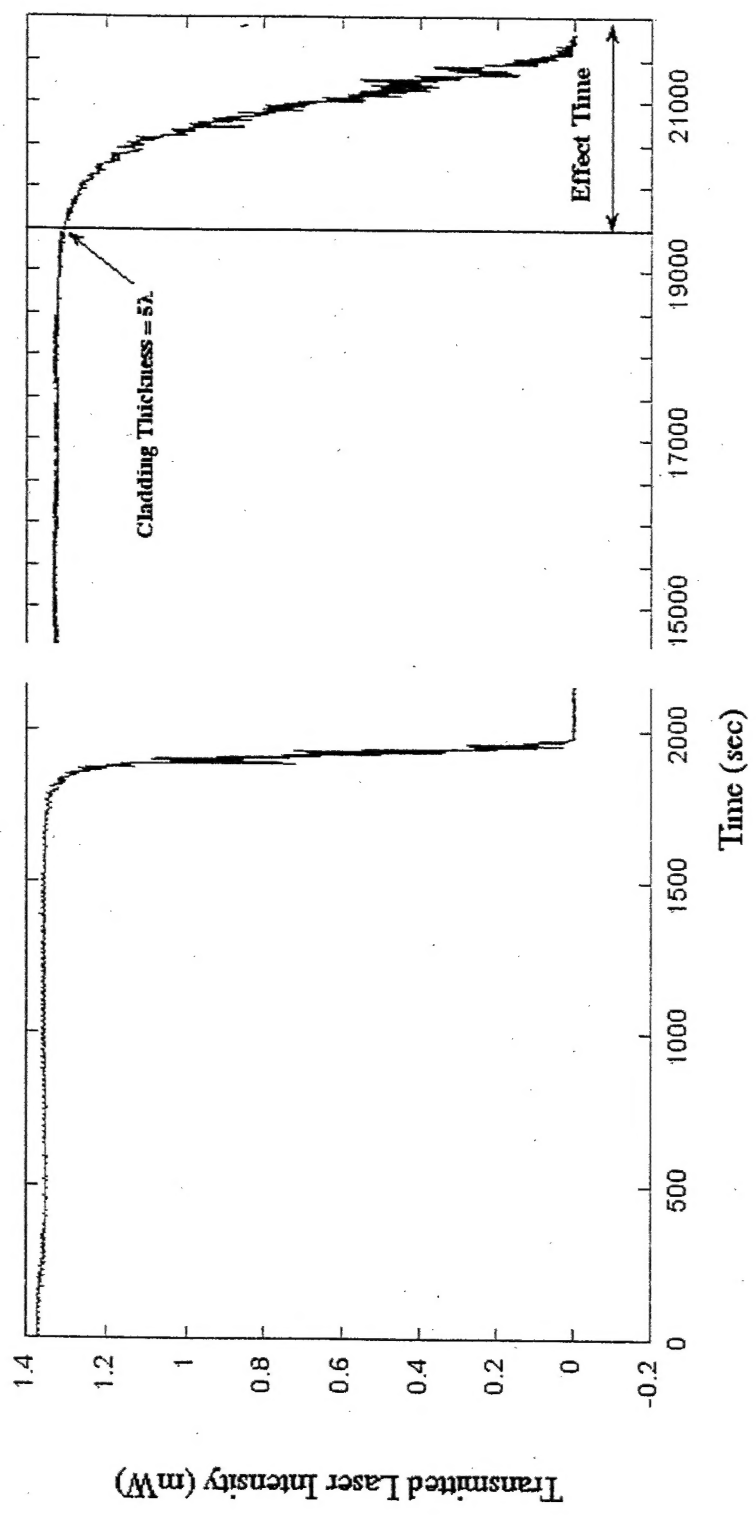


Figure 1.

Normalized Transmitted Intensity

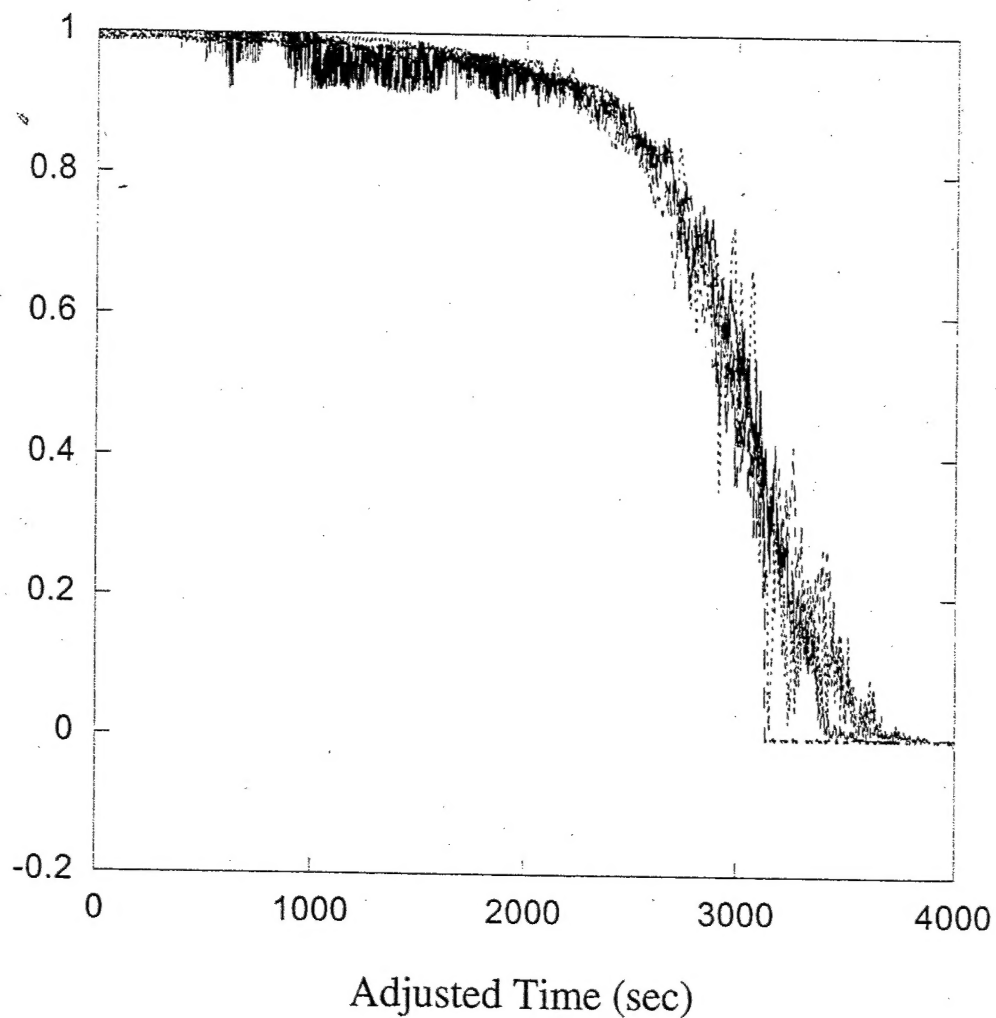


Figure 2.